NJC

Accepted Manuscript

Functionalization of silver nanoparticles with 5-sulfoanthranilic acid dithiocarbamate for selective colorimetric detection of Mn^{2+} and Cd^{2+} ions

Vaibhavkumar N. Mehta, Jigneshkumar V. Rohit and Suresh Kumar Kailasa[*]

Applied Chemistry Department, S. V. National Institute of Technology, Surat-395 007, India
[*]*Corresponding author, Phone: +91-261-2201730; Fax: +91-261-2227334*
E-mail: sureshkumarchem@gmail.com; skk@ashd.svnit.ac.in

Abstract

In this work, we have described the use of sulfoanthranilic acid dithiocarbamate functionalized silver nanoparticles as a probe for simple, rapid and simultaneous colorimetric detection of Mn^{2+} and Cd^{2+} ions. The Mn^{2+} and Cd^{2+} ions induce the aggregation of sulfoanthranilic acid dithiocarbamate functionalized silver nanoparticles, resulting a color change from yellow to orange associated with the red-shift in their surface plasmon resonance peak from 395 to 580 and 535 nm for Mn^{2+} and Cd^{2+} ions, respectively. Moreover, the aggregation of sulfoanthranilic acid dithiocarbamate functionalized silver nanoparticles induced by Mn^{2+} and Cd^{2+} ions was confirmed by dynamic light scattering and transmission electron microscopy. The Mn^{2+} and Cd^{2+} ions detection method based on surface plasmon resonance peak by UV-visible spectrophotometer offers wide linear detection ranges from 5 to 50 µM and 10 to 100 µM with the detection limits of 1.7 and 5.8 µM for Mn^{2+} and Cd^{2+} ions, respectively. The sulfoanthranilic acid dithiocarbamate functionalized silver nanoparticles act as a simple colorimetric probe for the simultaneous detection of Mn^{2+} and Cd^{2+} ions in various environmental water samples (drinking, tap, canal and river water) with good recovery values at minimal volume of samples.

Keywords: SAA-DTC-Ag NPs, Mn^{2+} ion, Cd^{2+} ion, UV-visible spectroscopy, DLS and TEM.

Introduction

Recently, heavy metal pollution in air, water and soil has become an important issue due to their toxic effects on living system.[1] Some of the metal ions (Cu^{2+}, Mn^{2+}, Ni^{2+}, Zn^{2+} and Fe^{3+}) are essentially required for living organisms, and play vital roles in different biological processes. Furthermore, manganese ion (Mn^{2+}) is one of the important element to biota and human being because its important role in the bone and other tissue formations, endogenous antioxidant enzymes, such as catalase and superoxide dismutases and also in the metabolism process of carbohydrate and lipids.[2,3] Moreover, the deficiency of Mn^{2+} can delay blood coagulation and hyper-cholesterolaemia in human body whereas the higher concentration of Mn^{2+} in human body can cause neurological disorder which results into the Parkinson's disease.[2,4] According to the U.S. Environmental Protection Agency (EPA) and Indian standard drinking water specification, the maximum permissible limit of manganese in drinking water is 300 and 100 μg/L.[5-6] Cadmium ion (Cd^{2+}) is one of the toxic element at trace levels which are extensively present in water, soil, air and sediment due to its widespread use in industry and agriculture. Furthermore, Cd^{2+} ion can easily accumulate in ecosystem and organisms *via* food chain and causes to damage various organs including lung, liver, kidney, bone, cardiovascular system and immune system since it has a long biological half-life of around 30 years.[7] According to the US EPA and World Health Organization (WHO), the highest desirable limits of cadmium in drinking water are 5.0 and 3.0 μg/L.[5,8] Therefore, the trace identification of both ions in environmental and food samples with minimized sample preparations has great significance. To date, there are many classical analytical techniques used for the detection of both ions (Mn^{2+} and Cd^{2+}) in environmental and biological samples such as atomic absorption spectrometry,[9]

inductively coupled plasma mass spectrometry,[10,11] inductively coupled plasma-atomic emission spectrometry,[12,13] fluorescence spectroscopy,[14] and graphite furnace atomic absorption spectrometry.[15] It is apparent that these methods expensive sophisticated instrumentations or complicated procedures, which makes them inconvenient for routine analysis of both metal ions. To meet the environmental protection agencies and to satisfy the requirement of an *on-site* real-time monitoring of both ions, the development of a facile, simple, selective and sensitive method is still urgently necessary for the trace identification of both ions in environmental samples at minimal volume of samples.

Recent years, metallic (Au and Ag) NPs-based colorimetric assay has drawn much more attention in the selective and sensitive detection of a wide variety chemical species in complex samples without the need for any complicated equipment.[16] Since Au and Ag NPs act as efficient selective colorimetric probes because of their distance-dependent optical properties and possess extremely high extinction coefficients at visible region.[17] The surface Plasmon resonance (SPR) of the above NPs changes dramatically upon the addition of target analytes, resulting a red-shift in their unique SPR and a change in color, corresponding to their dispersion and aggregation states, respectively.[18] Based on this, numerous Au and Ag NPs-based colorimetric methods have been developed for the selective and sensitive detection of metal species in various environments. Among Au and Ag NPs, Ag NPs exhibited many advantages over Au NPs including higher extinction coefficient (10^{10} M^{-1} cm^{-1}), higher ratio of scattering to extinction and sharper extinction bands which makes them more prominent candidate than Au NPs for colorimetric assays.[19,20] For example, Zhou *et al.* developed a colorimetric assay for Mn^{2+} ion in drinking water samples using 4-mercaptobenzoic acid (MBA) and melamine (MA) bifunctionalized Ag NPs as a probe with the detection limit of 5×10^{-8} M.[21] Wu's group illustrated

the use of tripolyphosphate (TPP) functionalized Ag NPs as a colorimetric probe for the detection of Mn^{2+} ion in lake and tap water samples.[22] The Au NPs were functionalized with *L*-dopa and successfully used as a colorimetric probe for the selective detection of Mn^{2+} ion.[23] Li *et al.* described the use of β-cyclodextrin (β-CD) functionalized Ag NPs as a probe for the colorimetric detection of Mn^{2+} ion in river water samples.[24] Similarly, Xue's group developed a colorimetric approach for the detection of Cd^{2+} ion in lake water samples using 6-mercaptonicotinic acid (MNA) and *L*-cysteine (Cys) bifunctionalized Au NPs as a probe.[25] Wang *et al.* illustrated the use of 4-amino-3-hydrazino-5-mercapto-1,2,4-triazole (AHMT) modified Au NPs as a probe for colorimetric sensing of Cd^{2+} ion in environmental water samples.[26] A colorimetric probe was developed based on the unmodified Au NPs for the detection of Cd^{2+} ion in water and digested rice samples.[27] A simple, low-cost and selective colorimetric assay was developed for the rapid detection of Cd^{2+} ion using 5-sulfosalicylic acid (SAA) functionalized Ag NPs as a probe.[28] Sung and Wu functionalized Au NPs with di-(1H-pyrrol-2-yl)methanethione (DP) and used as a probe for colorimetric detection of Cd^{2+} ion in lake water.[29] These reports suggested that the functionalized Au and Ag NPs can be effectively employed as colorimetric probes for the detection of either Mn^{2+} or Cd^{2+} ions in various environmental samples. Therefore, it is in great demand to develop Au and Ag NPs based colorimetric probe for the discriminative detection of multiple metal ions in various environmental and biological samples. In this connection, only limited approaches have been explored on the use of Au and Ag NPs as probes for the colorimetric detection of more than one metal ion in various environmental samples. For example, Ye *et al.* functionalized Au NPs with peptide (CALNNDHHHHHH) for simultaneous colorimetric detection of Cd^{2+}, Ni^{2+} and Co^{2+} ions in river water samples.[30] Rajendiran's group successfully illustrated the use of *L*-tyrosine-stabilized

Au and Ag NPs as colorimetric probes for the detection of Hg^{2+}, Pb^{2+} and Mn^{2+} ions in aqueous medium.[31] Most recently, Ag NPs were successfully synthesized from plant extracts (neem leaf, mango leaf, green tea and pepper seed) and used as colorimetric probes for parallel detection of Hg^{2+}, Zn^{2+} and Pb^{2+} ions in water samples.[32] Moreover, Anthony *et al.*developed a colorimetric probe based on *N*-(2-hydroxybenzyl)-valine (VP) and *N*-(2-hydroxybenzyl)-isoleucine (ILP) functionalized Ag NPs for simultaneous detection of Cd^{2+}, Hg^{2+} and Pb^{2+} ions in polluted ground water samples.[33] Wu and co-workers functionalized Ag NPs with stabilized with sodium pyrophosphate ($Na_4P_2O_7$) and hydroxypropylmethylcellulose (HPMC) and used as a colorimetric probe for the rapid detection of Cu^{2+} and Mn^{2+} ion at pH 1.9 and 12.0.[34] Recently, we have developed chitosan dithiocarbamate functionalized Au NPs as a probe for single metal ion (Cd^{2+} ion) detection with good selectivity.[35] These reports suggested that the functionalized Au and Ag NPs efficiently act as colorimetric probes for the sensitive multiple-metal ion detection in various environmental samples. So far, no reports are presented for the parallel detection of Mn^{2+} and Cd^{2+} ions by using functionalized Ag NPs as a colorimetric probe. Therefore, sulfoanthranilic acid dithiocarbamate (SAA-DTC) was functionalized on Ag NPs and used as a probe for the trace identification of more than one metal ion with good selectivity and sensitivity.

In this study, we developed a new Ag NPs-based colorimetric sensor that can be used for the detection of Mn^{2+} and Cd^{2+} ions. The Ag NPs are functionalized with SAA-DTC and the both Mn^{2+} and Cd^{2+} ions are induced the aggregation of SAA-DTC-Ag NPs, yielding in a color change of the solution from yellow to orange for Mn^{2+} and Cd^{2+} ion. In addition, compared to other published articles,[23,27,34] the present method shows more improvements as follows: (i) functionalization of Ag NPs is very simple, (ii) the good selectivity and sensitivity for Mn^{2+} and Cd^{2+} ions, and (iii) the LODs of Mn^{2+} and Cd^{2+} ion are significantly improved. The aggregation

of SAA-DTC-Ag NPs may be attributed to the complex formation between negatively charged

sulfonic group and Mn^{2+} and Cd^{2+} ions at PBS pH 8.0 (Scheme 1).
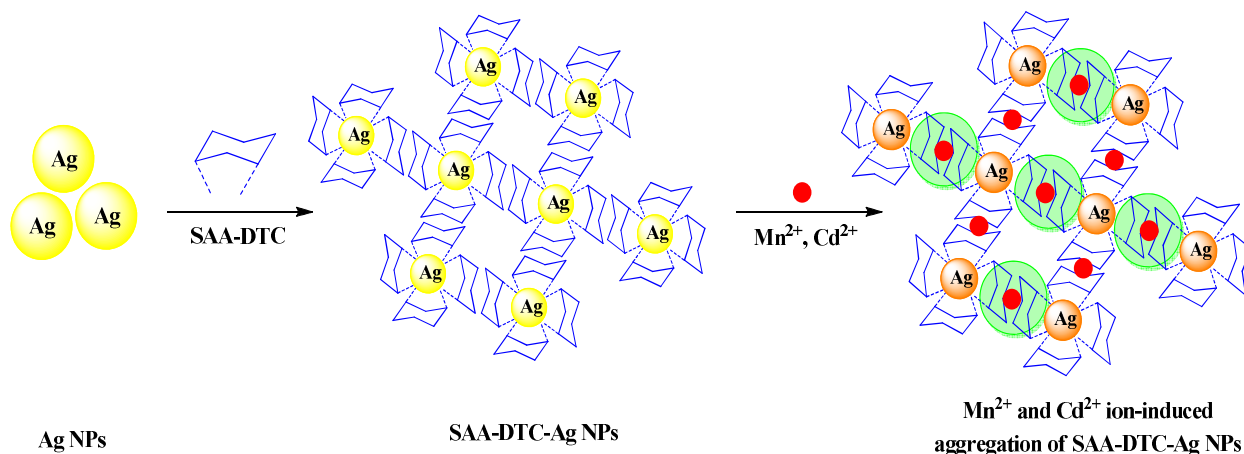
Scheme 1. Schematic representation of Mn^{2+} and Cd^{2+} ions-induced aggregation of SAA-DTC-Ag NPs.

Experimental

Chemicals and materials

Silver nitrate, sodium borohydride, 5-sulfoanthranillic acid and metal salts

$(Zn(NO_3)_2 \cdot 6H_2O, \quad Mn(NO_3)_2 \cdot 4H_2O, \quad Co(NO_3)_2 \cdot 6H_2O, \quad Pb(NO_3)_2, \quad Cd(NO_3)_2 \cdot 4H_2O,$

$Cu(NO_3)_2 \cdot 3H_2O, \; Hg(NO_3)_2 \cdot H_2O, \; FeCl_2 \cdot 4H_2O, \; Mg(NO_3)_2 \cdot 6H_2O, \; NiSO_4 \cdot 6H_2O, \; FeCl_3 \cdot 6H_2O,$

$Cr(NO_3)_2 . 6H_2O$ and $Na_2S_2O_4$) were purchased from Sigma-Aldrich, USA. Ethanol, carbon

disulfide, Na_2HPO_4, K_2HPO_4 and sodium chloride were obtained from Merck Ltd., India. All

chemicals were of analytical grade and used without further purification. Milli-Q-purified water

was used for the sample preparations.

Synthesis of SAA-DTC functionalized Ag NPs

The SAA-DTC was prepared by ultrasonic treatment of 1.0 mM SAA with equimolar mixture of ethanolic CS_2 for 20 min. The Ag NPs were synthesized according to the previously reported method with minor modification.[36] Briefly, 0.02 M of $AgNO_3$ and 0.5 mL of 1.0 mM sodium citrate were added into 4.0 mL of SAA-DTC solution, the mixture was diluted to 100 mL with the distilled water and then stirred for another 5 min following by the addition of 10 mg $NaBH_4$ into the mixture. The resultant mixture was allowed to stirr for another 1 h at room temperature to acquire molecular self-assembly of SAA-DTC on the surface of Ag NPs. The synthesized SAA-DTC-Ag NPs was stored in refrigerator at 4°C before use in all experiments. Figure 1 illustrates the synthesis procedure for the SAA-DTC and functionalization of SAA-DTC on the surface of Ag NPs.
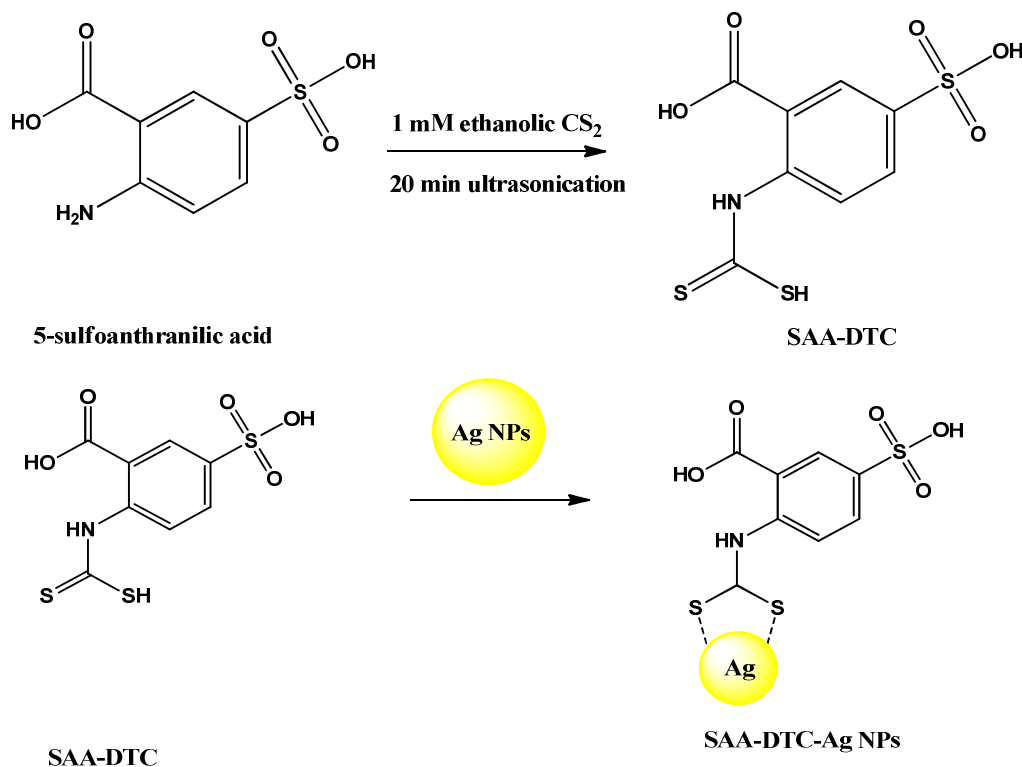

Figure 1. Schematic representation for synthesis of SAA-DTC and SAA-DTC-Ag NPs.

Colorimetric detection of Mn^{2+} and Cd^{2+} ions using SAA-DTC-Ag NPs as a probe

Colorimetric detection of Mn^{2+} and Cd^{2+} was carried out by adding 200 µL of different concentrations (5.0 – 100 µM) of Mn^{2+} and Cd^{2+} ions in 1.5 mL of SAA-DTC-Ag NPs in the presence of 100 µL PBS at pH 8.0, respectively. Then, the mixture was vortexed for 1 min and allowed to incubate at room temperature under optimal condition. The color change was observed from yellow to orange after addition of Mn^{2+} and Cd^{2+} ions. Subsequently, UV-visible absorption spectra of the above solutions were measured by using a Maya Pro 2000 spectrophotometer.

Detection of Mn^{2+} and Cd^{2+} ions in environmental water samples

The practical applicability of the proposed method was investigated by spiking the different concentrations of Mn^{2+} ion (5.0, 25 and 50 µM) and Cd^{2+} ion (10, 50 and 100 µM) with the various environmental water samples (i.e. drinking, tap, canal and river water). The drinking and tap water was collected from the research laboratory, SVNIT, Surat. The canal and river water samples were collected from the agriculture canal (Surat) and Tapi river (Surat), respectively. The collected water samples were filtered through the 0.45 µm filter and then spiked with the standard solutions of Mn^{2+} (5.0, 25 and 50 µM) and Cd^{2+} (10, 50 and 100 µM) ions and then analyzed by the above described procedure.

Instrumentation

UV-visible spectra were measured with Maya Pro 2000 spectrophotometer (Ocean Optics, USA) at room temperature. Fourier transform infrared (FT-IR) spectra were recorded on a Perkin Elmer (FT-IR spectrum BX, Germany). ^{1}H NMR spectra were taken on a Varian 400 MH$_Z$ instrument (USA). TEM samples were prepared by dropping 10-20 µL of SAA-DTC-Ag NPs colloidal solution onto a copper grid (3 mm, 200 mesh) coated with carbon film and allowed

it to dried up following by the analyzed with Tecnai 20 (Philips, Holland) transmission electron

microscope at an acceleration voltage of 100 kV. Dynamic light scattering (DLS) analysis was

performed on a Malvern Instruments Zetasizer Nano ZS90 (Malvern, UK) instrument for

characterization of the size distribution of nanoparticles in solution.

Results and discussion

Characterization of SAA-DTC-Ag NPs

Before the characterization of SAA-DTC-Ag NPs, the effect of SAA-DTC concentration

(0.5 to 3.0 mM) on the surface of Ag NPs was investigated since the capping agent concentration

play important role in the colorimetric detection by providing the active binding sites for the

complexation with the target analytes. It was observed that the SPR peak of Ag NPs was greatly

influenced by the addition of different concentration of SAA-DTC. As shown in Supporting

Information of Figure S1a, the characteristic SPR peak of bare Ag NPs at 390 nm was red-

shifted towards longer wavelength as the concentration increases from 1.5 to 3.0 mM,

confirming that the aggregation of Ag NPs, which leads a color change form yellow to orange.

However, the absorption spectra and color of Ag NPs did not show any changes by addition the

concentration of SAA-DTC in the range of 0.5 - 1.0 mM, which indicates that the stability of Ag

NPs. Supporting Information of Figure S1b shows the UV-visible spectra of bare Ag NPs before

and after functionalization with 1.0 mM of SAA-DTC concentration. It can be seen that the

minor red-shift in SPR peak of bare Ag NPs was observed at 395 nm after functionalization with

1.0 mM of SAA-DTC concentration. This red-shift may be attributed to the attachment of SAA-

DTC on the surface of Ag NPs *via* thiolate linkage which results into a change in dielectric

constant of the microenvironment around the nanoparticles.[37] Moreover, Ag NPs still remain in

the dispersion state with uniform size and stability due to the electrostatic repulsion between negatively charged sulfo groups of SAA-DTC-Ag NPs.[38] Therefore, we selected 1.0 mM of SAA-DTC as an optimal concentration for the functionalization of Ag NPs.

The functionalization of Ag NPs with SAA-DTC was further confirmed by FT-IR and ^{1}H NMR spectroscopic techniques. Supporting Information of Figure S2 shows the FT-IR spectra of pure 5-sulfoanthranillic acid, SAA-DTC and SAA-DTC-Ag NPs. FT-IR spectrum of pure 5-sulfoanthranillic acid shows two characteristic bands at 3484 and 3013 cm^{-1} correspond to N–H and O-H asymmetric and symmetric stretching modes, respectively. The strongest absorption band at 1216 cm^{-1} is ascribed to C-N stretching mode. The band at 871 cm^{-1} belongs to aromatic C-H stretching. The bands at 1740 and 1344 cm^{-1} are ascribed to the stretching vibrations of C=O and S=O groups in SAA-DTC, respectively. As shown in Supporting Information of Figure S2b, FT-IR spectrum of SAA-DTC exhibits the new peaks for the stretching vibrations of C-S, -S-H and CS-NH groups at 1086, 2504 and 1282 cm^{-1}, respectively. Supporting Information of Figure S2c shows the FT-IR spectrum of SAA-DTC-Ag NPs. It can be observed that –S-H group stretching and bending modes were not observed at 2504 cm^{-1} in the spectrum of SAA-DTC-Ag NPs due to the successful attachment of SAA-DTC on the surface of Ag NPs *via* thiolate linkage.

Supporting Information of Figure S3 shows the ^{1}H NMR spectra of pure 5-sulfoanthranillic acid, SAA-DTC and SAA-DTC-Ag NPs. As shown in Supporting Information of Figure S3a, the peaks at 7.0–8.2 δ ppm correspond to the aromatic protons of sulfoanthranillic acid. The peak at 5.5 δ ppm corresponds to the proton of –NH$_2$ of SAA. Furthermore, the broad peak at 9.4 δ ppm corresponds to the integration of –OH and –SO$_3$H groups of SAA. The new peak of –SH group is observed at 1.2 δ ppm due to the formation of DTC derivative of SAA

(Supporting Information of Figure S3b). Moreover, the disappearance of –SH group peak at 1.2 δ ppm is due to the molecular assembly of SAA-DTC on the surface of Ag NPs *via* carbodithioate linkage (Supporting Information of Figure S3c).

The hydrodynamic diameter of SAA-DTC-Ag NPs was estimated in response from the autocorrelation function of the intensity of light scattered from the particles *via* Brownian motion.[39] As shown in Figure 2, bare Ag NPs were monodispersed with an average hydrodynamic diameter of ~5.6 nm. After modification of Ag NPs with SAA-DTC, the average hydrodynamic diameter of Ag NPs was increased to ~ 20 nm (Figure 2b), indicating that the functionalization of SAA-DTC on the surface of Ag NPs, which leads to the increase in whole nanoparticle or aggregate population on the surface.[40] Furthermore, the surface morphology of SAA-DTC-Ag NPs was also investigated by TEM. Figure 3a-b represents TEM images of SAA-DTC-Ag NPs at scale bars 100 and 20 nm. These results indicate that the SAA-DTC molecules on Ag NPs are important to reduce the chemical interface effects on the plasmon resonance, preventing the Ag NPs aggregation and reducing the surface energy to counterbalance thermodynamic driving forces, which allows particle size to be more directly controlled and well dispersed in aqueous media.
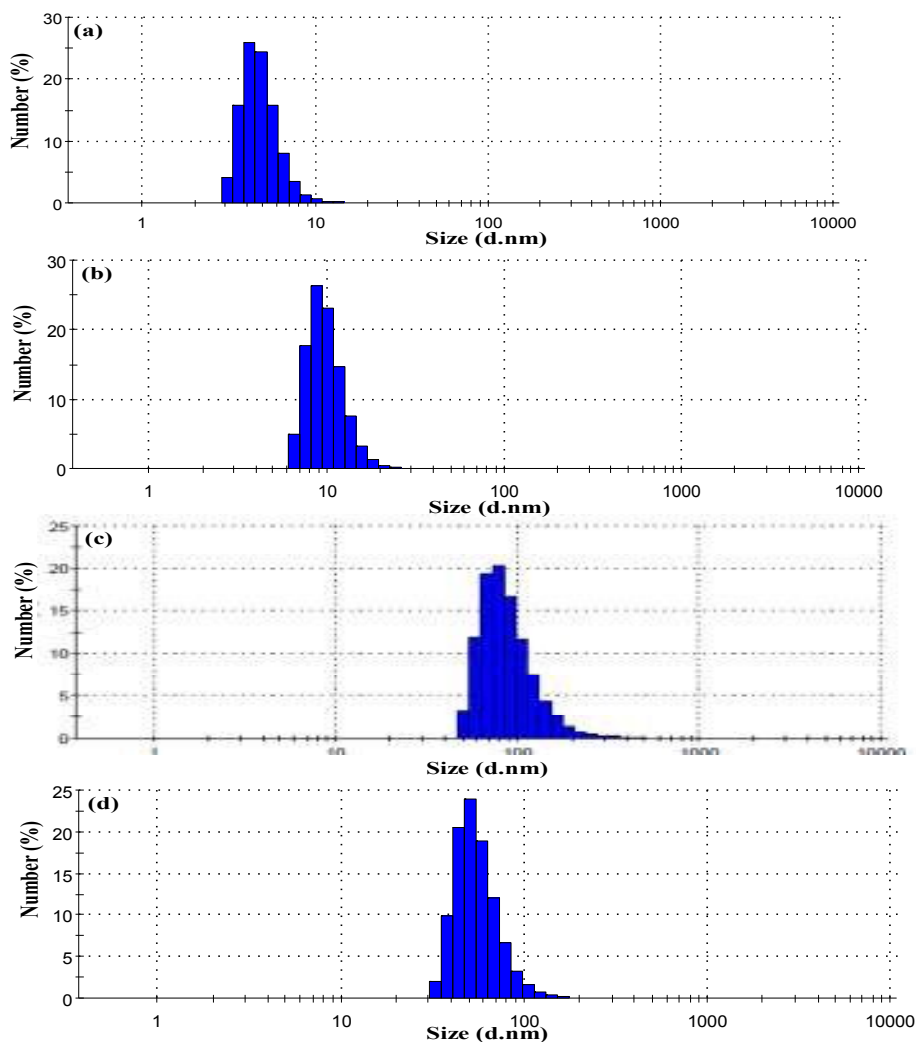
Figure 2. DLS analysis of (a) bare Ag NPs (b) SAA-DTC-Ag NPs and the aggregation of SAA-DTC-Ag NPs induced by (c) Mn^{2+} and (d) Cd^{2+} ions.

UV-visible spectroscopy is one of the simplest characterization techniques to determine particle formation and its stability. As we know that the spectrum surface plasmon resonance of NPs is influenced by the size, shape, interparticle interactions, free electron density and surrounding medium, which indicates that it is an efficient tool for monitoring the stability of Ag NPs. As shown in Supporting Information of Figure S4, the SPR peak of SAA-DTC-Ag NPs at 395 nm was almost observed with same intensity from 1st day to 7th day, indicating that the

SAA-DTC-functionalized Ag NPs are stable for long time, which confirms that the surface
modification of Ag NPs with SAA-DTC prevents aggregation of Ag NPs thereby leading stable
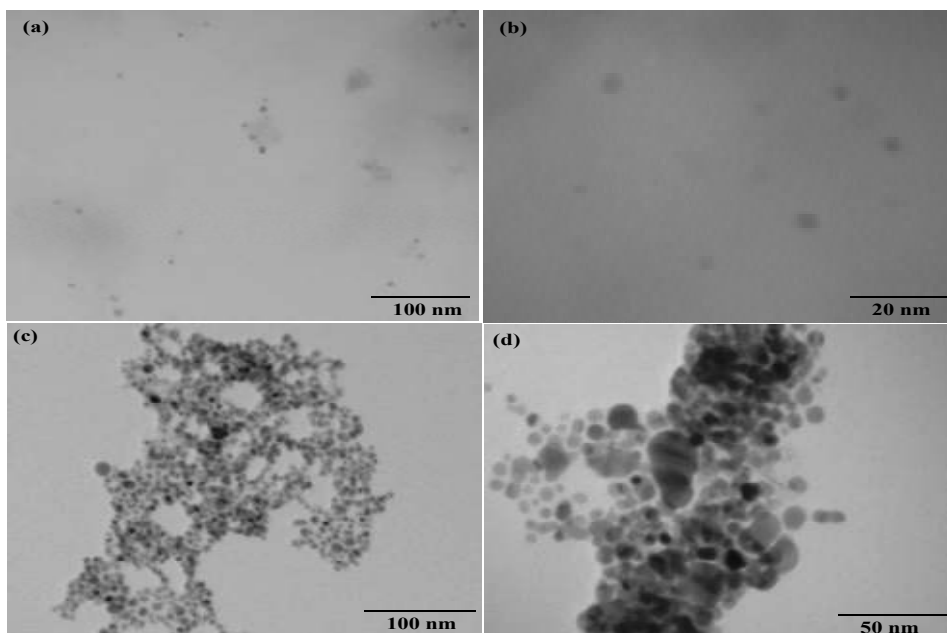Ag NPs solution for long time without any spectral or color changes.

Figure 3. TEM images of SAA-DTC-Ag NPs at scale bars (a) 100 nm and (b) 20 nm and the
aggregation of SAA-DTC-Ag NPs induced by the addition of (c) Mn^{2+} (50 μM) and (d)
Cd^{2+}(100 μM) ions.

Sensing ability of SAA-DTC-Ag NPs for metal ions recognition

The selectivity of SAA-DTC-Ag NPs towards different metal ions was also investigated. Briefly, 200 μL of different metal ions solution (Cd^{2+}, Co^{2+}, Cr^{3+}, Cu^{2+}, Fe^{2+}, Fe^{3+}, Hg^{2+}, Mn^{2+}, Mg^{2+}, Na^+, Ni^{2+}, Pb^{2+} and Zn^{2+}, 100 μM) were added separately into 1.5 mL of SAA-DTC-Ag NPs at PBS pH 8.0 and their corresponding UV-visible absorption spectra were measured. Figure 4 shows the UV-visible spectra and color of SAA-DTC-Ag NPs after addition of different metal ions. It was clearly observed that the SPR peak of SAA-DTC-Ag NPs was decreased at 395 nm and new peaks were generated at 580 nm and 535 nm for Mn^{2+} and Cd^{2+} ions, respectively, whereas other metal ions did not show any noticeable change in the SPR peak of SAA-DTC-Ag NPs (Figure 4a). As shown in Figure 4b, only Mn^{2+} and Cd^{2+} ions induce the aggregation of SAA-DTC-Ag NPs with the color change from yellow to orange among all the metal ions. These results confirm that the selectivity of SAA-DTC-Ag NPs is good towards Mn^{2+} and Cd^{2+} ions over other metal ions. Furthermore, Mn^{2+} and Cd^{2+} ions induced SAA-DTC-Ag NPs aggregation was also confirmed by DLS and TEM. As shown in Figure 2c and d, the average hydrodynamic diameter of SAA-DTC-Ag NPs was increased from ~20 nm to ~255 and ~ 190 nm after addition Mn^{2+} and Cd^{2+} ions, which is due to the aggregation of SAA-DTC-Ag NPs induced by Mn^{2+} and Cd^{2+} ions. Figure 3c and d shows the TEM images of Mn^{2+} and Cd^{2+} ions induced aggregation of SAA-DTC-Ag NPs. It was observed that the morphology of SAA-DTC-Ag NPs was changed from monodisperse to polydisperse due to the aggregation of SAA-DTC-Ag NPs induced by Mn^{2+} and Cd^{2+} ions.
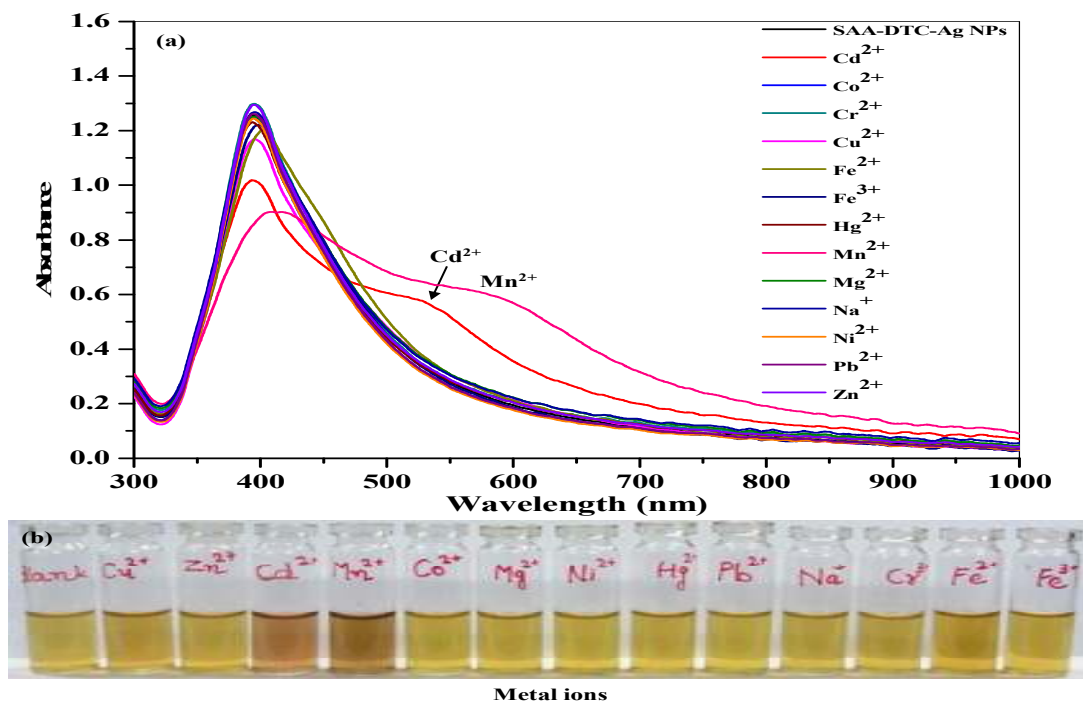
Figure 4. (a) UV-visible absorption spectra of SAA-DTC-Ag NPs in the presence of different metal ions (Cd^{2+}, Co^{2+}, Cr^{3+}, Cu^{2+}, Fe^{2+}, Fe^{3+}, Hg^{2+}, Mn^{2+}, Mg^{2+}, Na^+, Ni^{2+}, Pb^{2+} and Zn^{2+}, 100 μM) and (b) Photographic image of SAA-DTC-Ag NPs in the presence of the above metal ions.

Effect of pH on the recognition of Mn^{2+} and Cd^{2+} ions

The stability of SAA-DTC-Ag NPs was investigated by using PBS at different pH 2.0-12. At pH 2.0 and 3.0, absorption ratio (A_{535nm}/A_{395nm}) of SAA-DTC-Ag NPs was quite higher without addition of analyte, which confirm the aggregation of SAA-DTC-Ag NPs in acidic pH at < 4.0 (Supporting Information of Figure S5). The aggregation of Ag NPs at lower pH may be

15

attributed to the decrease in the interparticle distance between the neighboring nanoparticles due

to the surface charge neutralization of sulfonic groups leading to red shift of SPR peak.[41]

Furthermore, no noticeable change was observed in the absorption ratio (A_{535nm}/A_{395nm}) of SAA-

DTC-Ag NPs at pH $\geq$ 4.0. Therefore, SAA-DTC-Ag NPs were stable in pH range of 5.0 - 12,

and can be used as the suitable range for colorimetric detection of Mn^{2+} and Cd^{2+} ions. The effect

of pH on the aggregation of SAA-DTC-Ag NPs in presence of Mn^{2+} and Cd^{2+} ions was also

investigated and shown in Supporting Information of Figure S5. The electron destiny of $-SO_3H$

group decreased at lower pH values (pH < 5.0) which hinders the complexation of metal ions

with sulfonic groups.[42] At higher pH values (pH > 9.0), the coordination ability between the

metal ions and SAA-DTC-Ag NPs was decreased due to the metal hydroxide formation.

Moreover, the absorption ratios (A_{580nm}/A_{395nm} and A_{535nm}/A_{395nm}) were higher at pH 8.0 after

addition of Mn^{2+} and Cd^{2+} ions, which confirms the high degree of SAA-DTC-Ag NPs

aggregation due to the donor-acceptor interaction between the negatively charged $-SO_3H$ groups

and positively charged Mn^{2+} and Cd^{2+} ions. Therefore, pH 8.0 was considered as the best pH for

the further colorimetric detection of metal ions.

Mechanism for the simultaneous colorimetric detection of Mn^{2+} and Cd^{2+} ions by SAA-DTC-Ag NPs

As shown in Figure 1, 5-sulfoanthranillic acid contains the amino ($-NH_2$) and sulfonic

group ($-SO_3H$) which provides the binding sites for the metal ions to form the coordination

complexation. It can be noticed that amino groups have already involved in the formation of

dithiocarbamate groups which felicitate the attachment of SAA-DTC on the surface of Ag NPs.

Therefore, -SO₃H groups are only groups available for the complexation with the metal ions. Moreover, the oxygen atom of negatively charged sulfonate group possesses the capacity to bridge more than one positively charged metal center.[43] Therefore, Mn^{2+} and Cd^{2+} ions make the coordination complex due to the intermolecular charge transfer between negatively charged sulfonate groups of SAA-DTC-Ag NPs and both the metal ions *via* donor-acceptor interactions. Based on the hypothesis, this complexation leads to the decrease in the interparticle distance between the nearby nanoparticles which results a red-shift in their SPR peak from 395 nm to 580 and 535 nm for Mn^{2+} and Cd^{2+} ions, respectively, yielding a color change from yellow to orange.

Effect of NaCl on the stability and sensitivity

It is well known that the addition of NaCl as ionic strength accelerates the aggregation process of NPs due to the colloidal instability, rendering higher sensitivity. In this connection, first we studied the effect of NaCl concentration from 0.001 to 1.0 M on the UV-visible absorption spectra of SAA-DTC-Ag NPs. The UV-visible absorption spectra of SAA-DTC-Ag NPs show a reduction of the absorbance at 395 nm concomitant with NaCl rising concentrations, indicating that the aggregation of SAA-DTC-Ag NPs at high ionic strength. However, the absorption spectra of SAA-DTC-Ag NPs did not cause any change at 0.1 M of NaCl, which indicates the prevention of aggregate formation in NaCl as ionic strength (Supporting Information of Figure S6). In order to know the influence of NaCl on the aggregation of SAA-DTC-Ag NPs induced by both Mn^{2+} and Cd^{2+} ion, we studied the UV-visible absorption of spectra of SAA-DTC-Ag NPs upon the addition of 1.0 mM both ions separately in the presence of 0.1 M NaCl (Supporting Information of Figure S7). It can be noticed that the SPR peak at 395 nm was not red-shifted and the color of the solution was not changed upon the addition of both

ions in the presence of NaCl, indicating that the both ions did not induce the aggregation of SAA-DTC-Ag NPs in the presence of NaCl, which confirms the released Ag^+ binds with excess Cl^- in the solution, forming AgCl. As a result, AgCl can precipitate onto the surface of Ag NPs and create a surface in which the Ag NPs would no longer repel each other or interact with other chemical species,[44] which leads to neutral surface conditions and creates a lack of steric hindrance.[45] These results indicate that the application of the probe was greatly affected in the presence of NaCl as ionic strength. However, both ions are effectively induced the aggregation of SAA-DTC-Ag NPs without NaCl, resulting a red-shift in their spectra and a change in color from yellow to orange. Based on these observations, we carried out the sensitivity experiment without addition of NaCl.

Sensitivity study for simultaneous colorimetric detection of Mn^{2+} and Cd^{2+} ions by SAA-DTC-Ag NPs

The UV-visible absorption spectra and colorimetric response are used to further evaluate the sensitivity of SAA-DTC-Ag NPs-based sensor system. To this, a series of different concentration of Mn^{2+} (5.0 to 50 µM) and Cd^{2+} (10 to 100 µM) ions were added separately into SAA-DTC-Ag NPs solutions, respectively. Figures 5a and 6a show the UV-visible spectra of SAA-DTC-Ag NPs upon the addition of different concentrations of Mn^{2+} (05 to 50 µM) and Cd^{2+} (10 to 100) at PBS pH 8.0. With the increase of both ions (Mn^{2+} and Cd^{2+}) concentrations, the SPR peak at 395 nm gradually decreases, accompanied with the appearance of two new SPR peaks at 580 and 535 nm for Mn^{2+} and Cd^{2+} ions those going up quickly (Figures 5b and 6b). These results confirm that the higher concentration of Mn^{2+} and Cd^{2+} ions induce higher degree of SAA-DTC-Ag NPs aggregation. Figures 5b and 6b show the color change of SAA-DTC-Ag

NPs form yellow to orange with increasing concentrations of Mn^{2+} and Cd^{2+} ions, respectively. It indicates that the SAA-DTC-Au NPs aggregates with the increase of concentration both ions, and the color change from yellow to orange with increasing Mn^{2+} and Cd^{2+} ions concentrations can be observed.
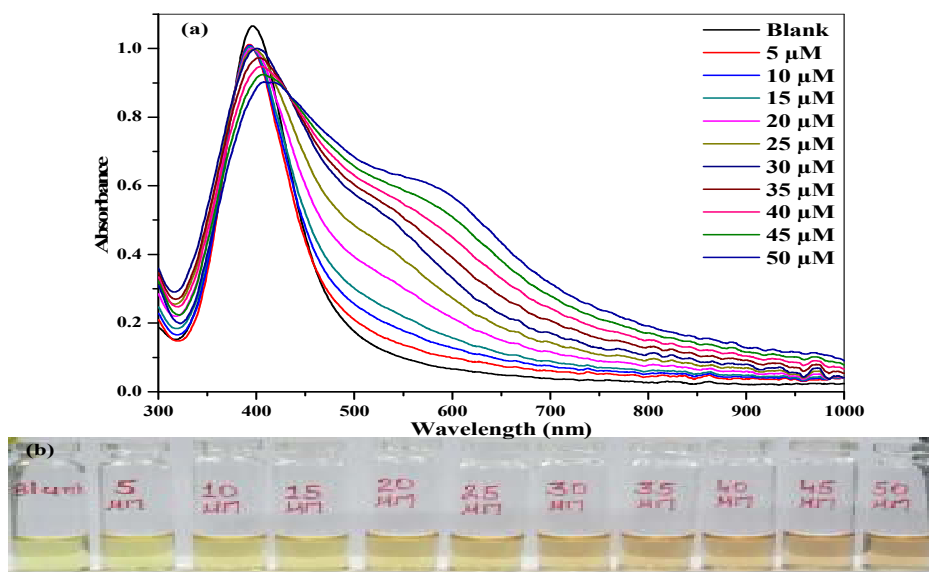

Figure 5. (a) UV-visible absorption spectra of SAA-DTC-Ag NPs with different concentrations of Mn^{2+} ion in the range of 5.0 to 50 μM and (b) photographic image of SAA-DTC-Ag NPs with the addition of different concentrations of Mn^{2+} ion from 5.0 to 50 μM.

Furthermore, the absorption ratios at A_{580nm}/A_{395nm} and A_{535nm}/A_{395nm} were used to plot the calibration graphs for Mn^{2+} and Cd^{2+} ions in order to calculate the detection limits. The absorbance ratios at A_{580nm}/A_{395nm} and A_{535nm}/A_{395nm} show linear response towards both ions in the range from 5.0 to 50 μM ($R^2 = 0.9862$) and 10 to 100 μM ($R^2 = 0.9973$) for Mn^{2+} and Cd^{2+} ions, respectively (Supporting Information of Figure S8). From the calibration graph, the detection limits were found to be 1.7 and 5.8 μM for Mn^{2+} and Cd^{2+} ions, which are lower than that of the reported methods[23,34] and comparable with reported methods based on metallic NPs.[27] Importantly, the obtained LODs (0.18 and 1.33 μg/L for Mn^{2+} and Cd^{2+} ions) are all lower than the standard of WHO (300 and 3.0 μg/L for Mn^{2+} and Cd^{2+} ions) and US-EPA (5.0 μg/L for Cd^{2+} ion) drinking water standards. The analytical performance of the present method was compared with several other methods for the detection of Mn^{2+} and Cd^{2+} in the literature (Table 1). Evidently, the present method involves simple procedure for the functionalization of Ag NPs, and allows us to detect both ions (Mn^{2+} and Cd^{2+}) simultaneously and conveniently. Therefore, the present method provides a simple platform for on-site, real time simultaneous detection of Mn^{2+} and Cd^{2+} ions without using multiple colorimetric probes for each metal ion.
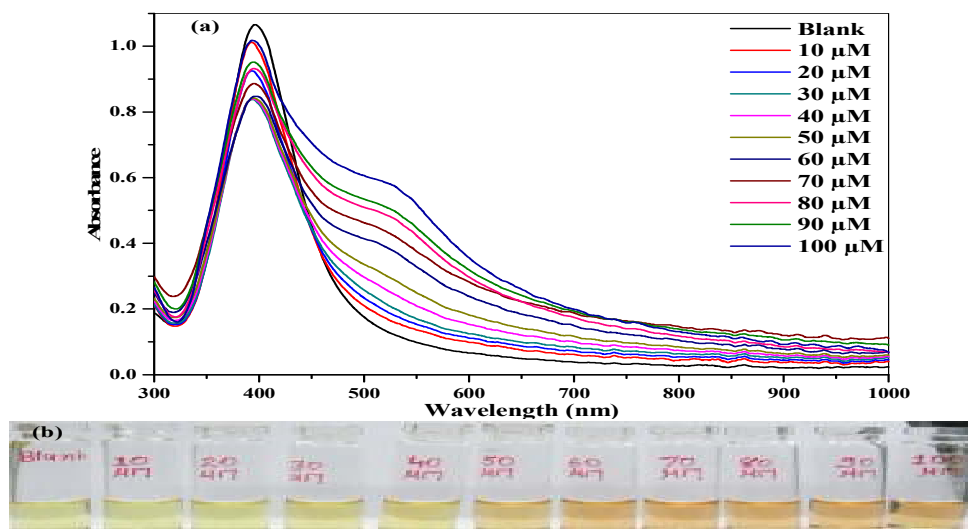
Figure 6. (a) UV-visible absorption spectra of SAA-DTC-Ag NPs with different concentrations of Cd^{2+} ion in the range of 10 to 100 μM and (b) photographic image of SAA-DTC-Ag NPs with the addition of different concentrations of Cd^{2+} ion from 10 to 100 μM.

Interference study

Detection of Mn^{2+} and Cd^{2+} ions in environmental and food samples requires assessment of SAA-DTC-Ag NPs-sensor selectivity towards both ions in the presence of other possibly reactive sample matrix components. To confirms this, we carried out competitive experiments by adding mixture of metal ions (Co^{2+}, Cr^{3+}, Cu^{2+}, Fe^{2+}, Fe^{3+}, Hg^{2+}, Mg^{2+}, Na^+, Ni^{2+}, Pb^{2+} and Zn^{2+}, 500 μM) in presence of Mn^{2+} and Cd^{2+} ions (100 μM). As shown in Figure 7, SAA-DTC-Ag

NPs did not show any spectral and color change with addition of mixture of metal ions. Moreover, only Mn^{2+} and Cd^{2+} ions are induced the color change from yellow to orange, resulting a red-shift in the SPR peak. These results demonstrated that the other metal ion did not induce the aggregation of SAA-DTC-Ag NPs, confirms the high selectivity of SAA-DTC-Ag NPs towards Mn^{2+} and Cd^{2+} ions. The good selectivity for Mn^{2+} and Cd^{2+} ions ascribe to the formation of the coordination compounds by both ions with carboxylic and sulfonic groups of SAA-DTC-Ag NPs at PBS pH 8.0, which results in the aggregation of SAA-DTC-Ag NPs. Therefore, the SAA-DTC-Ag NPs can be suitable for detecting Mn^{2+} and Cd^{2+} in environmental and food samples at minimal volume of samples.
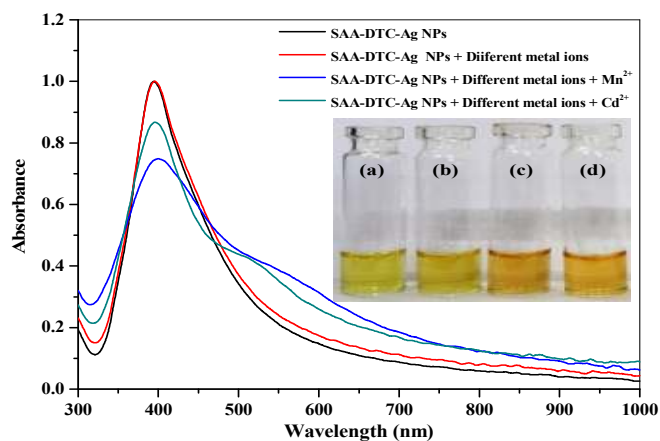
Figure 7. UV-visible absorption spectra of (a) SAA-DTC-Ag NPs (b) SAA-DTC-Ag NPs in the presence of different metal ions (Co^{2+}, Cr^{3+}, Cu^{2+}, Fe^{2+}, Fe^{3+}, Hg^{2+}, Mg^{2+}, Na^+, Ni^{2+}, Pb^{2+} and Zn^{2+}, 500 µM) without Mn^{2+} and Cd^{2+} ions (c) SAA-DTC-Ag NPs in the presence of Mn^{2+} ion and (d) SAA-DTC-Ag NPs in the presence of Cd^{2+} ion along with different metal ions (Co^{2+}, Cr^{3+}, Cu^{2+}, Fe^{2+}, Fe^{3+}, Hg^{2+}, Mg^{2+}, Na^+, Ni^{2+}, Pb^{2+} and Zn^{2+}).

Analysis of Mn^{2+} and Cd^{2+} ions in environmental water samples

In order to evaluate the practical applicability of the proposed method, different environmental water samples (drinking, tap, river and canal) were spiked with different concentration of Mn^{2+}(5, 25 and 50 µM) and Cd^{2+} (10, 50 and 100 µM) ions and then analyzed by the aforesaid procedure. The percentage recovery and relative standard deviation are shown in Table 2 (*n*=3). The proposed method shows good recovery values in the range of 98.16 - 100.45% and 98.42 - 101.22%, with the % RSD values 0.82 - 1.77% and 1.07 - 1.93% for Mn^{2+} and Cd^{2+} ions in various environmental water samples. Therefore, the present method can provide a facile platform for discriminative detection Mn^{2+} and Cd^{2+} ions in environmental water samples with good accuracy and precision.

Conclusions

In summary, we successfully develop a facile, selective and rapid colorimetric method for simultaneous detection of Mn^{2+} and Cd^{2+} ion using SAA-DTC-Ag NPs as a probe. The method involves simple procedures for the functionalization of Ag NPs and does not need complicated operations, and it has fast response rate and good selectivity. The Mn^{2+} and Cd^{2+} ions induce the rapid aggregation of SAA-DTC-Ag NPs *via* coordinate covalent bonds between Mn^{2+} and Cd^{2+} ions and carboxylic and sulfo groups of SAA-DTC-Ag NPs, resulting in a color change, which can be easily observed by the naked eye. The detection limits were found to be 1.7 and 5.8 µM

for Mn^{2+} and Cd^{2+} ions, which is lower than the WHO and US-EPA. This probe does not require any solvents or special additives. The SAA molecular assembly on Ag NPs may provide effective binding sites and good coordination conditions that make them as potential candidates for capturing of Mn^{2+} and Cd^{2+} ion selectively. The SAA-DTC-Ag NPs based colorimetric probe may offer pronounced advantage for simultaneous and discriminative detection of Mn^{2+} and Cd^{2+} ions in various environmental water samples.

Acknowledgement

References

1. R. F. Pasternack and P. J. Collings, *Science*, 1995, **269**, 935-939.

2. World Health Organization, Trace Elements in Human Nutrition and Health,1996, **163**.

3. J. R. Wispe, B. B. Warner, J. C. Clark, C. R. Dey, J. Neuman, S. W. Glasser, J. D. Crapo, L. Y. Chang and J. A. Whitsett, *J. Biol. Inorg. Chem.,* 1992, **267**, 23937-23941.

4. G. Oszlanczi, T. Vezer, L. Sarkozi, E. Horvath, Z. Konya and A. Papp, *Ecotox. Environ. Safe* , 2010, **73**, 2004-2009.

5. U.S. EPA. Health Effects Support Document for Manganese. EPA 822-R-03-003. Washington, DC: U.S. Environmental Protection Agency; 2003

6. Bureau of Indian Standards Drinking Water Specification, 1st Revision, ISS 10500 (1991).

7. D. M. Templeton and Y. Liu, *Chem. Biol. Interact.*, 2010, **188**, 267-275.

8. World Health Organization (WHO), Guidelines for Drinking Water Quality, Health Criteria and Other Supporting Information, World Health Organization, Geneva, 2nd edn, 1998, vol. 2.

9. A. Malekpour, S. Hajialigol and M. A .Taher, *J. Hazard. Mater.*, 2009, **172**, 229-233.

10. D. Beauchemin and S. S. Berman, *Anal. Chem.,*1989, **61**, 1857-1862.

11. W. Guo, S. Hu, Y. Xiao, H. Zhang and X. Xie, *Chemosphere*, 2010, **81**, 1463-1468.

12. A. Matsumoto, S. Osaki, T. Kobata, B. Hashimoto, H. Uchihara and T. Nakahara, *Microchem. J.*, 2010, **95**, 85-89.

13. C. R. Lan and Z. B. Alfassi, *Analyst,* 1994, **119**, 1033-1035.

14. S. Yunus, S. Charles, F. Dubois and E. V. Donckt, *J. Fluoresc.*, 2008, **18**, 499-506.

15. M. G. A. Korn, G. L. dos Santos, S. M. Rosa, L. S. G. Teixeira and P. V. de Oliveira, *Microchem. J.*, 2010, **96**, 12-16.

16. K. Saha, S. S. Agasti, C. Kim, X. Li and V. M. Rotello, *Chem. Rev.*, 2012, **112**, 2739–2779.

17. K. Aslan, J. R. Lakowicz and C. D. Geddes, *Anal. Biochem*., 2004, **330,** 145-155.

18. S. K. Ghosh and T. Pal, *Chem. Rev*., 2007, **107**, 4797–4862.

19. T. C. Prathna, N. Chandrasekaran, A. M. Raichur and A. Mukherjee, *Colloids Surf. B*, 2011, **82,** 152-159.

20. J. S. Lee, A. K. R. L. Jean, S. J. Hurst and C. A. Mirkin, *Nano Lett.,* 2007, **7**, 2112-2115.

21. Y. Zhou, H. Zhao, C. Li, P. He, W. Peng, L. Yuan, L. Zeng and Y. He, *Talanta*, 2012, **97**, 331-335.

22. Y. X. Gao, J. W. Xin, Z. Y. Shen, W. Pan, X. Li and A.G. Wu, *Sens. Actuat. B,* 2013, **181**, 288-293.

23. K. B. Narayanan and H. H. Park, *Spectrochim. Acta A*, 2014, **131**, 132-137.

24. R. Hu, L. Zhang and H. Li, *New J. Chem.*, 2014, **38**, 2237-2240.

25. Y. Xue, H. Zhao, Z. Wu, X. Li, Y. He and Z. Yuan, *Analyst*, 2011, **136**, 3725-3730.

26. A. J. Wang , H. Guo, M. Zhang, D. L. Zhou, R. Z. Wang and J. J. Feng, *Microchim Acta,* 2013 **180**, 1051-1057.

27. Y. Guo, Y. Zhang, H. Shao, Z. Wang, X. Wang and X. Jiang, *Anal. Chem.*, 2014, **86**, 8530−8534.

28. W. Jin, P. Huang, F. Wu and L. H. Ma, *Analyst*, 2015, **140**, 3507–3513.

29. Y. M. Sung, and S. P. Wu, *Sens. Actuat. B*, 2014, **201**, 86–91.

30. M. Zhang, Y. Q. Liu and B. C. Ye, *Analyst*, 2012, **137**, 601-607.

31. M. Annadhasan, T. Muthukumarasamyvel, V. R. Sankar Babu and N. Rajendiran, *ACS Sustainable Chem. Eng.*, 2014, **2**, 887-896.

32. D. Karthiga and S. P. Anthony, *RSC Adv.*, 2013, **3**, 16765-16774.

33. V. Vinod Kumar and S. P. Anthony, *Sens. Actuators, B*, 2014, **191**, 31-36.

34. G. Wu, C. Dong, Y. Li, Z. Wang, Y. Gao, Z. Shen and A. Wu, *RSC Adv.*, 2015, **5**, 20595–20602.

35. V. N. Mehta, H. Basu, R. K. Singhal and S. K. Kailasa, *Sens. Actuators B*, 2015, **220**, 850–858.

36. H. Cao, M. Wei, Z. Chen and Y. Huang, *Analyst*, 2013, **138**, 2420-2426.

37. Y. H. Su, S. H. Chang, L. G. Teoh, W. H. Chu and S. L. Tu, *J. Phys. Chem. C*, 2009, **113**, 3923–3928.

38. Z. Sun, Z. Cui and H. Li, *Sens. Actuators, B*, 2013, **183**, 297– 302.

39. X. Liu, Q. Dai, L. Austin, J. Coutts, G. Knowles, J. Zou, H. Chen and Q. Huo, *J. Am. Chem. Soc.,* 2008, **130**, 2780-2782.

40. Q. Wang, L. Yang, X. Yang, K. Wang and J. Liu, *Analyst*, 2013, **138**, 5146-5150.

41. A. Mocanu, I. Cernica, G. Tomoaia, L. D. Bobos, O. Horovitz, M. Tomoaia-Cotisel, *Colloids Surf., A*, 2009, **338**, 93-101.

42. Y. Shang, D. Gao, F. Wu and X. Wan, *Microchimica Acta*, 2013, **180**, 1317-1324.

43. T. Z. Forbes and S. C. Sevov, *Inorg. Chem.*, 2009, **48**, 6873–6878.

44. S. K. Mwilu, A. M. El Badawy, K. Bradham, C. Nelson, D. Thomas, K. G. Scheckel, T. Tolaymat, L. Z. Ma, K. R. Rogers, *Sci. Total Environ.*, 2013, **447**, 90−98.

45. J. L. Axson, D. I. Stark, A. L. Bondy, S. S. Capracotta, A. D. Maynard, M. A. Philbert, I. L. Bergin, and A. P. Aul, *J. Phys. Chem. C*, 2015, **119**, 20632–20641.

Figure captions

Scheme 1. Schematic representation of Mn^{2+} and Cd^{2+} ions-induced aggregation of SAA-DTC-Ag NPs.

Figure 1. Schematic representation for synthesis of SAA-DTC and SAA-DTC-Ag NPs.

Figure 2. DLS analysis of (a) bare Ag NPs (b) SAA-DTC-Ag NPs and the aggregation of SAA-DTC-Ag NPs induced by (c) Mn^{2+} and (d) Cd^{2+} ions.

Figure 3. TEM images of SAA-DTC-Ag NPs at scale bars (a) 100 and (b) 20 nm and the aggregation of SAA-DTC-Ag NPs induced by the addition of (c) Mn^{2+} (50 μM) and (d) Cd^{2+} (100 μM) ions.

Figure 4. (a) UV-visible absorption spectra of SAA-DTC-Ag NPs in the presence of different metal ions (Cd^{2+}, Co^{2+}, Cr^{3+}, Cu^{2+}, Fe^{2+}, Fe^{3+}, Hg^{2+}, Mn^{2+}, Mg^{2+}, Na^+, Ni^{2+}, Pb^{2+} and Zn^{2+}, 100 μM) and (b) Photographic image of SAA-DTC-Ag NPs in the presence of the above metal ions.

Figure 5. (a) UV-visible absorption spectra of SAA-DTC-Ag NPs with different concentrations of Mn^{2+} ion in the range of 5.0 to 50 μM and (b) photographic image of SAA-DTC-Ag NPs with the addition of different concentrations of Mn^{2+} ion from 5.0 to 50 μM.

Figure 6. (a) UV-visible absorption spectra of SAA-DTC-Ag NPs with different concentrations of Cd^{2+} ion in the range of 10 to 100 μM and (b) photographic image of SAA-DTC-Ag NPs with the addition of different concentrations of Cd^{2+} ion from 10 to 100 μM.

Figure 7. UV-visible absorption spectra of (a) SAA-DTC-Ag NPs (b) SAA-DTC-Ag NPs in the presence of different metal ions (Co^{2+}, Cr^{3+}, Cu^{2+}, Fe^{2+}, Fe^{3+}, Hg^{2+}, Mg^{2+}, Na^+, Ni^{2+}, Pb^{2+} and Zn^{2+}, 500 μM) without Mn^{2+} and Cd^{2+} ions (c) SAA-DTC-Ag NPs in the presence of Mn^{2+} ion and (d) SAA-DTC-Ag NPs in the presence of Cd^{2+} ion along with different metal ions (Co^{2+}, Cr^{3+}, Cu^{2+}, Fe^{2+}, Fe^{3+}, Hg^{2+}, Mg^{2+}, Na^+, Ni^{2+}, Pb^{2+} and Zn^{2+}).

Table 1. Comparison of SAA-DTC-Ag NPs as a colorimetric probe for the detection of Mn^{2+} and Cd^{2+} ions with the reported methods on Au and Ag NPs as probes.

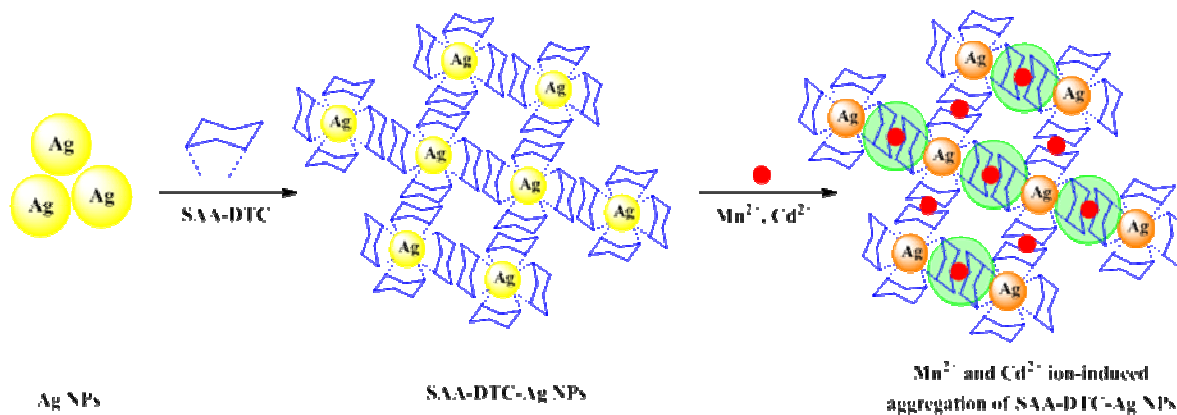| NPs	Capping agent	Analytes	LOD (M)	Merits and demerits	Reference
Ag NPs	4-MBA and MA	Mn^{2+}	5.0×10^{-8}	The LOD is lower, however required tedious steps for functionalization. It is a single metal ion sensor.	[21]
Ag NPs	TPP	Mn^{2+}	0.1×10^{-6}	The LOD is good, but it is single metal ion sensor.	[22]
Au NPs	*L*-dopa	Mn^{2+}	$<5.0 \times 10^{-6}$	The LOD is higher, however required tedious steps for functionalization and single metal ion sensor.	[23]
Ag NPs	β-CD	Mn^{2+}	5.0×10^{-7}	The LOD is reasonable and single metal ion sensor. It requires multiple steps.	[24]
Au NPs	MNA and Cys	Cd^{2+}	1.0×10^{-7}	The LOD is good, and single metal ion sensor. Two steps are involved in the functionalization of Au NPs.	[25]
Au NPs	AHMT	Cd^{2+}	30×10^{-9}	The LOD is lower, but it is single metal ion sensor.	[26]
Au NPs	-	Cd^{2+}	5.0×10^{-6}	The LOD is similar to the present method, but it is single metal ion sensor. Poor selectivity.	[27]
Ag NPs	SAA	Cd^{2+}	3.0×10^{-9}	The LOD is higher and it is single metal ion sensor.	[28]
Au NPs	DP	Cd^{2+}	16.6×10^{-9}	The LOD is higher and it is single metal ion sensor.	[29]
Au NPs	Peptide	Cd^{2+}	0.05×10^{-6}	Synthesis of peptides is tedious.	[30]
Ag NPs	VP and ILP	Cd^{2+}	1.0×10^{-6}	Reasonable LOD and required two Ag NPs systems.	[33]
Ag NPs	$Na_4P_2O_7$ and HPMC	Mn^{2+}	1.8×10^{-6}	Higher LOD and required two reagents.	[34]
Ag NPs	SAA-DTC	Mn^{2+} Cd^{2+}	1.7×10^{-6} 5.8×10^{-6}	Lower LODs than the WHO and US EPA, sensing two metal ions.	Present study

Table 2. SAA-DTC-Ag NPs as a colorimetric probe for the detection of Mn^{2+} and Cd^{2+} ions in spiked environmental water samples (drinking, tap, canal and river water).

Sample	Mn^{2+}				Cd^{2+}			
	Added (μM)	Found (μM)	Recovery (%)[a]	RSD (%)[a]	Added (μM)	Found (μM)	Recovery (%)[a]	RSD (%)[a]
Drinking	5	4.98	99.78	1.77	10	9.90	99.05	1.12
	25	25.03	100.13	1.27	50	49.72	99.44	1.07
	50	50.22	100.45	0.82	100	101.22	101.22	1.03
Tap	5	4.99	99.90	1.75	10	9.88	98.88	1.19
	25	25.02	100.10	1.27	50	49.51	99.02	1.81
	50	50.20	100.40	1.29	100	100.14	100.14	1.34
Canal	5	4.95	99.10	1.74	10	9.84	98.42	1.93
	25	24.91	99.66	1.24	50	49.23	98.46	1.36
	50	49.08	98.16	1.75	100	99.79	99.79	1.07
River	5	4.96	99.22	1.54	10	9.87	98.70	1.52
	25	24.94	99.79	1.23	50	49.21	98.43	1.35
	50	49.98	99.96	1.30	100	99.83	98.83	1.10

[a](n=3)

Graphical abstract

Sulfoanthranilic acid dithiocarbamate molecular assembly was carried on Ag NPs for simple, rapid and simultaneous colorimetric detection of Mn^{2+} and Cd^{2+} ions with less interference at minimal volume of sample.

Schematic representation of Mn^{2+} and Cd^{2+} ions-induced aggregation of SAA-DTC-Ag NPs.